Communications in Mathematics and Applications
Vol. 14, No. 4, pp. 1405–1419, 2023
ISSN 0975-8607 (online); 0976-5905 (print)
Published by RGN Publications
DOI: 10.26713/cma.v14i4.2578

http://www.rgnpublications.com

***Special Issue*:**
Recent Trends in Applied and Computational Mathematics
Proceedings of the Third International Conference on Recent Trends in Applied and Computational Mathematics (ICRTACM-2022)
School of Applied Sciences, Department of Mathematics,
Reva University, Bangaluru, India, 10th & 11th October, 2022
***Editors*: M. Vishu Kumar, A. Salma, B. N. Hanumagowda and U. Vijaya Chandra Kumar**

Research Article

Linear and Non-Linear Analysis of Rayleigh-Bénard Convection in a Micropolar Fluid Occupying Enclosures With Realistic Boundaries

Sandra Jestine*[1] and S. Pranesh[2]

Department of Mathematics, CHRIST (deemed to be University), Bangalore, India
*__Corresponding author:__ sandra.jestine@res.christuniversity.in

Received: January 28, 2023 **Accepted:** May 24, 2023

Abstract. The linear and non-linear analysis of *Rayleigh-Bénard convection* (RBC) in a *micropolar fluid* (MPF) occupying enclosures are analyzed for realistic boundaries. The different enclosures considered are shallow enclosure ($h < b$), square enclosure ($h = b$) and tall enclosure ($h > b$). Linear analysis is conducted to study the on-set-of-convection, using the Fourier series representation. The different boundaries taken into consideration are Free-Free (F-F), Rigid-Free (R-F) and Rigid-Rigid (R-R). Using the Fourier-series representation, the fourth order Lorenz model is derived to quantify the heat transport. The effect of various MPF parameters has been analyzed. The rate of heat transfer is calculated from average Nusselt number, ($\overline{\mathcal{N}u(t)}$).

Keywords. Micropolar fluid, Rayleigh-Bénard convection, Enclosure, Realistic boundaries

Mathematics Subject Classification (2020). 76A02, 76M15

1. Introduction

In the early time, describing the characteristics of fluid with micro-elements was challenging. The classical Navier-Stokes model failed to incorporate the effect of micro-rotation of suspended-elements. A. C. Eringen ([6, 7]) proposed theory of micropolar fluid, which is a subclass of microfluids. The micropolar fluid equations are derived by taking into account the micro-rotation of suspended-elements, that resulted in addition of one extra equation to classical Newtonian model — conservation of angular momentum. These fluids are considered non-Newtonian because of the presence of micro-elements that rotate on their own axis altering the fluid's behaviour. The early insights concerning the study on Rayleigh-Bénard convection in a micropolar fluid began by Datta and Sastry [4], Ahmadi [1], Rao [17], Bhattacharyya and Jena [2], Payne and Straughan [15], and Qin and Kaloni [16].

Siddheshwar and Pranesh [22] investigated magneto-convection in a micropolar fluid. The study reveals that, comparison of electrically conducting Newtonian-fluid with micropolar fluid, the fluid with micro-elements is more stable. The other important works on micropolar fluid can be seen on the works of Siddheswar and Pranesh [21]. Considering various applications of micropolar fluid, Sastry *et al*. [19] studied drug delivery in cardiovascular-system, where they considered blood particles as micropolar particles and drug carrier particles as nanoparticles.

Enclosures are finite spaces that are bounded and filled with liquids or gases. Internal convection is yet another term for natural convection in enclosures. Natural convection in enclosures has become one of the active area for current research due to it's several applications in the field of engineering. The early incites on flow inside a rectangular cavity is explored by authors Gill [9], Ostrach [13], Kimura and Bejan [11], Trevisan and Bejan [25], Gelfgat [8], and D'Orazio *et al*. [5]. The heat transfer characteristics of buoyancy-driven nanofluids inside rectangular enclosures with differentially heated vertical walls are investigated theoretically by Corcione [3]. It's interesting to note that increasing the aspect ratio of the enclosure enhances heat transfer.

Rayleigh-Bénard convection in Newtonian liquids-nanoliquids occupying different enclosures was investigated by Siddheshwar and Kanchana [20]. They used the multiscale method to convert Lorenz-model to a tractable GLE (*Ginzburg-Landau Equation*), whose solution measures the heat-transport. Kanchana *et al*. [10] conducted an analytical investigation of Rayleigh-Bénard convection in four types of enclosures in NIFR (*non-inertial frame of reference*). The NIFR effect resulted a stable system and thereby reduced heat-transport. The other recent works on enclosures can be seen in Mikhailenko [12], Santos *et al*. [18], and Olayemi *et al*. [14].

Unsteady-natural-convection in an enclosure with liquid-saturated-porous medium using LTNE (*local thermal non-equilibrium*) is studied by Siddheshwar and Siddabasappa [23]. In their investigation, it is observed that, heat transfer is greatest in shallow and least in tall enclosure. Siddheshwar and Sushma [24] performed non-linear analysis of Rayleigh-Bénard convection for rigid isothermal boundaries. While comparing heat transfer, they discovered that the rigid isothermal boundary has less heat transfer rate than the free isothermal case.

There are no reported works on Rayleigh-Bénard convection in a micropolar fluid occupying enclosures with realistic boundaries. Therefore, the main objective of the paper is to study the linear and non-linear analysis of Rayleigh-Bénard convection in a micropolar fluid occupying enclosures with F-F, R-F, and R-R boundaries.

2. Mathematical Formulation

The physical configuration of the problem consists of (i) shallow, (ii) square and (iii) tall enclosures filled with micropolar fluid as shown in Figure 1. The horizontal boundaries at $z=-\frac{h}{2}$ and $z=+\frac{h}{2}$ are taken either as stress-free, no spin and isothermal or rigid, no-spin and isothermal or rigid-free, no-spin and isothermal. The vertical boundaries at $x=-\frac{b}{2}$ and $x=+\frac{b}{2}$ are taken as stress-free, no-spin and adiabatic or rigid, no-spin and adiabatic or rigid-free, no-spin and adiabatic. Temperatures are kept fixed at the bottom $(T_0+\Delta T)$ and the top (T_0) boundaries, where the temperature difference is ΔT (>0). All the parameters are taken independent of y-co-ordinate, as we limit ourselves to the xz-plane for mathematical tractability, with gravity acting vertically downwards.

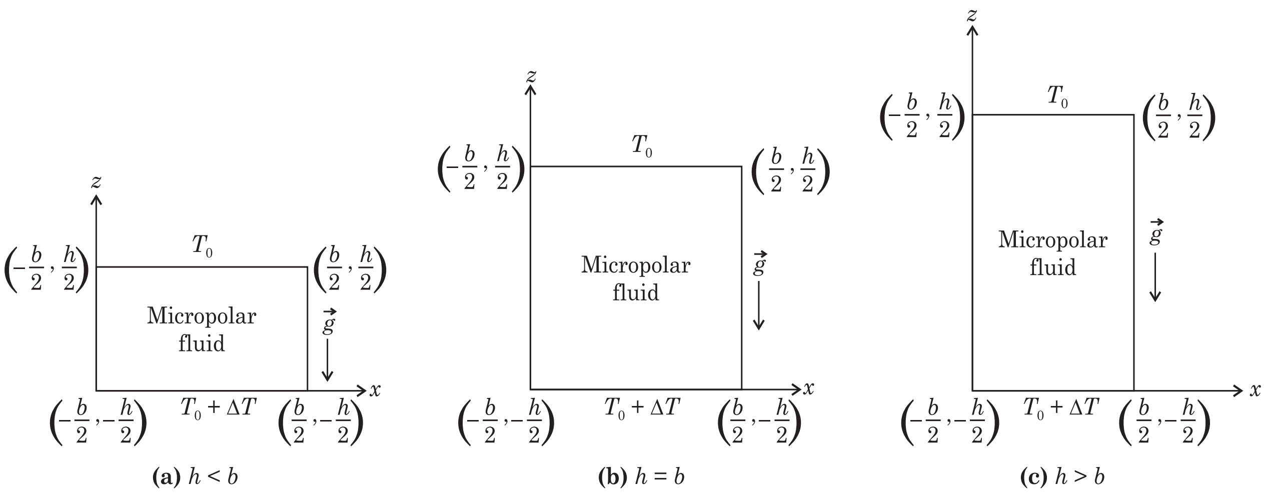

Figure 1. Physical representation of the problem with (a) shallow ($A_r<1$), (b) square ($A_r=1$), and (c) tall ($A_r>1$) enclosures

The basic equations that governs the problem modelled above are:

Conservation of Mass:

$$\nabla\cdot\vec{q}=0. \tag{2.1}$$

Conservation of Linear Momentum:

$$\varrho_o\left(\frac{\partial\vec{q}}{\partial t}+(\vec{q}\cdot\nabla)\vec{q}\right)=-(\nabla p)-(\varrho g)\hat{k}+(2\xi+\eta)\nabla^2\vec{q}+\xi(\nabla\times\vec{\omega}\ ). \tag{2.2}$$

Conservation of Angular Momentum:

$$\varrho_o I\left(\frac{\partial\vec{\omega}}{\partial t}+(\vec{q}\cdot\nabla)\vec{\omega}\right)=(\eta'+\lambda')\nabla(\nabla\cdot\vec{\omega})+\eta'\nabla^2\vec{\omega}+2\xi((\nabla\times\vec{q})-2\vec{\omega}). \tag{2.3}$$

Conservation of Energy:

$$\frac{\partial T}{\partial t}+(\vec{\mathfrak{q}}\cdot\nabla)T=\left(\frac{\beta}{\varrho_0 C_v}(\nabla\times\vec{\omega})\cdot\nabla T\right)+\chi\nabla^2 T. \tag{2.4}$$

Equation of State:

$$\varrho=\varrho_0(1-\alpha[T-T_0]). \tag{2.5}$$

The quantities in eqns. (2.1)–(2.5) are, $\vec{\mathfrak{q}}$: velocity, ϱ_0 : reference-density, $\mathfrak{p}$: pressure, g : gravitational-acceleration, ξ : coupling-viscosity-coefficient, ϱ : density, η : shear-kinematic-viscosity-coefficient, $\vec{\omega}$: angular-velocity, T : temperature, I : inertia, α : coefficient-of-thermal-expansion, β : micropolar-heat-conduction-parameter, η' and λ' : shear and bulk spin-viscosity-coefficients, and C_v : specific-heat.

In the motionless state, the quantities velocity, pressure, density, angular velocity and temperature are given by:

$$\vec{\mathfrak{q}}_b=(0,0),\quad \mathfrak{p}=\mathfrak{p}_b(z),\quad \varrho=\varrho_b(z),\quad \vec{\omega}_b=(0,0),\quad T=T_b(z). \tag{2.6}$$

Substituting eqn. (2.6) into eqns. (2.2), (2.4) and (2.5), we obtain the motionless state solutions as:

$$0=-\frac{d\mathfrak{p}_b}{dz}-\varrho_b g, \tag{2.7}$$

$$0=\frac{d^2T_b}{dz^2} \tag{2.8}$$

and

$$\varrho_b=\varrho_0[1-\alpha(T_b-T_0)], \tag{2.9}$$

where the subscript b denotes the motionless state. Eqns. (2.1) and (2.3) are satisfied by eqn. (2.6). Isothermal and adiabatic temperature conditions are assumed for horizontal and vertical boundaries respectively and are given by:

$$\left.\begin{array}{ll} T=T_0, & \text{at } z=+\frac{h}{2} \\ T=T_0+\Delta T, & \text{at } z=-\frac{h}{2} \end{array}\right\}-\frac{b}{2}<x<+\frac{b}{2}, \tag{2.10}$$

$$\left.\frac{\partial T}{\partial x}=0,\quad \text{at } x=-\frac{b}{2},+\frac{b}{2}\right\}-\frac{h}{2}<z<+\frac{h}{2}. \tag{2.11}$$

On solving eqn. (2.8) using constraints given in eqn. (2.10) yields,

$$T_b=\left[\frac{1}{2}-\frac{z}{h}\right]\Delta T+T_0. \tag{2.12}$$

The motionless state solutions are super imposed by an infinitesimal perturbation given by:

$$\left.\begin{array}{l} \vec{\mathfrak{q}}=\vec{\mathfrak{q}_b}+\vec{\mathfrak{q}}',\quad \mathfrak{p}=\mathfrak{p}_b+\mathfrak{p}',\quad \varrho=\varrho_b+\varrho', \\ \vec{\omega}=\vec{\omega}_b+\vec{\omega}',\quad T=T_b+T', \end{array}\right\} \tag{2.13}$$

where, prime, ($'$) represents the slight disturbance imposed on system. In order to lessen the number of variables bring in stream function, Ψ (for velocity component) that satisfies the continuity equation as follows:

$$u'=\frac{\partial}{\partial z}(\Psi')\quad \text{and}\quad w'=-\frac{\partial}{\partial x}(\Psi'). \tag{2.14}$$

Introduce the non-dimensional quantities as given below:

$$\left.\begin{array}{l}(x^*,z^*)=\left(\frac{x}{b},\frac{z}{h}\right),\quad \omega^*=\frac{\omega'}{(\chi/h^2)},\quad \Psi^*=\frac{\Psi'}{\chi},\\ T^*=\frac{T'}{\Delta T},\quad t^*=\frac{t}{(h^2/\chi)}.\end{array}\right\} \tag{2.15}$$

Substituting eqn. (2.13), introducing eqn. (2.14), applying eqn. (2.15) to resulting equation and neglecting the pressure term by cross-differentiation, we obtain the system of non-dimensional equations as:

$$\begin{bmatrix}(1+N_1)\nabla^4_{A_r} & -N_1\nabla^2_{A_r} & -Ra_{A_r}(A_r)^4\frac{\partial}{\partial x}\\ N_1\nabla^2_{A_r} & (N_3\nabla^2_{A_r}-2N_1) & 0\\ -(A_r)\frac{\partial}{\partial x} & -(A_r)N_5\frac{\partial}{\partial x} & \nabla^2_{A_r}\end{bmatrix}\begin{bmatrix}\Psi\\ \omega_y\\ T\end{bmatrix}$$

$$=\frac{\partial}{\partial t}\begin{bmatrix}\frac{1}{Pr}\nabla^2_{A_r}\Psi\\ \frac{N_2}{Pr}\omega_y\\ T\end{bmatrix}-\begin{bmatrix}\frac{A_r}{Pr}J(\nabla^2_{A_r}\Psi,\Psi)\\ A_r\frac{N_2}{Pr}J(\Psi,\omega_y)\\ (A_r)J(\Psi,T)-(A_r)N_5J(\omega_y,T)\end{bmatrix}, \tag{2.16}$$

where

$$\nabla_{A_r}=A_r\frac{\partial}{\partial x}\hat{i}+\frac{\partial}{\partial z}\hat{k},\quad J(\,,\,)=\text{Jacobian}.$$

The dimensionless quantities in eqn. (2.16) are given in Table 1.

Table 1. Dimensionless quantities

N_1	Coupling parameter	$\frac{\xi}{\eta+\xi}$
N_2	Inertia parameter	$\frac{1}{h^2}$
N_3	Couple stress parameter	$\frac{\eta'}{(\eta+\xi)h^2}$
N_5	Micropolar heat conduction parameter	$\frac{\beta}{\varrho_0 C_v h^2}$
Ra	Rayleigh number	$\frac{\alpha g\Delta T b^3\varrho_0}{(\eta+\xi)\chi}$
Pr	Prandtl number	$\frac{\eta+\xi}{\varrho_0\chi}$
A_r	Aspect ratio	$\frac{h}{b}$

3. Linear Stability Theory

In this subsection, the linear stability-analysis is discussed by eliminating the Jacobians in eqn. (2.16). The stationary-convection is performed on the system assuming principle of (exchange-of) stability to be valid. The linearized version of the equation take the form:

$$\begin{bmatrix}(1+N_1)\nabla^4_{A_r} & -N_1\nabla^2_{A_r} & -Ra(A_r)^4\frac{\partial}{\partial x}\\ N_1\nabla^2_{A_r} & (N_3\nabla^2_{A_r}-2N_1) & 0\\ -A_r\frac{\partial}{\partial x} & -A_rN_5\frac{\partial}{\partial x} & \nabla^2_{A_r}\end{bmatrix}\begin{bmatrix}\Psi\\ \omega_y\\ T\end{bmatrix}=0. \tag{3.1}$$

The stability of the system depends upon boundaries bounding the fluid. In this paper, the following boundary conditions on velocity and temperature are considered to inspect the stability.

1. *Horizontal Free-Free Isothermal* (HFFI) and *Vertical Free-Free Adiabatic* (VFFA)

$$\left.\begin{array}{ll}\Psi = \frac{\partial^2 \Psi}{\partial x^2} = \frac{\partial T}{\partial x} = 0, & \text{at } x = -\frac{1}{2}, \frac{1}{2}, \ -\frac{1}{2} < z < \frac{1}{2} \\ \Psi = \frac{\partial^2 \Psi}{\partial z^2} = T = 0, & \text{at } z = -\frac{1}{2}, \frac{1}{2}, \ -\frac{1}{2} < x < \frac{1}{2}\end{array}\right\} \tag{3.2}$$

2. *Horizontal Rigid-Free Isothermal* (HRFI) and *Vertical Rigid-Free Adiabatic* (VRFA)

$$\left.\begin{array}{ll}\Psi = \frac{\partial \Psi}{\partial x} = \frac{\partial T}{\partial x} = 0, & \text{at } x = -\frac{1}{2}, \ -\frac{1}{2} < z < \frac{1}{2} \\ \Psi = \frac{\partial^2 \Psi}{\partial z^2} = \frac{\partial T}{\partial x} = 0, & \text{at } x = +\frac{1}{2}, \ -\frac{1}{2} < z < \frac{1}{2}\end{array}\right\},$$

$$\left.\begin{array}{ll}\Psi = \frac{\partial \Psi}{\partial x} = T = 0, & \text{at } z = -\frac{1}{2}, \ -\frac{1}{2} < x < \frac{1}{2} \\ \Psi = \frac{\partial^2 \Psi}{\partial z^2} = T = 0, & \text{at } z = +\frac{1}{2}, \ -\frac{1}{2} < x < \frac{1}{2}\end{array}\right\} \tag{3.3}$$

3. *Horizontal Rigid-Rigid Isothermal* (HRRI) and *Vertical Rigid-Rigid Adiabatic* (VRRA)

$$\left.\begin{array}{ll}\Psi = \frac{\partial \Psi}{\partial x} = \frac{\partial T}{\partial x} = 0, & \text{at } x = -\frac{1}{2}, \frac{1}{2}, \ -\frac{1}{2} < z < \frac{1}{2} \\ \Psi = \frac{\partial \Psi}{\partial z} = T = 0, & \text{at } z = -\frac{1}{2}, \frac{1}{2}, \ -\frac{1}{2} < x < \frac{1}{2}\end{array}\right\} \tag{3.4}$$

The normal mode solutions of Ψ, ω_y and T satisfying the boundary conditions are assumed to take the form:

$$\left.\begin{array}{l}\Psi = \Psi_a \mathcal{G}_1(x,z), \\ \omega_y = \omega_{ya} \mathcal{G}_1(x,z), \\ T = T_a \mathcal{G}_2(x,z).\end{array}\right\} \tag{3.5}$$

The trial functions $\mathcal{G}_1(x,z)$ and $\mathcal{G}_2(x,z)$ are chosen such that it satisfies the eqns. (3.2)–(3.4) and are as shown in Table 2:

Table 2. Trial functions for linear analysis

F-F	R-F	R-R
$\mathcal{G}_1(x,z) = \cos(\pi x)\cos(\pi z)$	$\mathcal{G}_1(x,z) = S_f(x)\, S_f(z)$	$\mathcal{G}_1(x,z) = C_f(x)\, C_f(z)$
$\mathcal{G}_2(x,z) = \cos(\pi x)\sin(\pi z)$	$\mathcal{G}_2(x,z) = \cos(2\pi x)\sin(2\pi z)$	$\mathcal{G}_2(x,z) = \sin(\pi x)\cos(\pi z)$
—	$\mu = 7.85320462$	$\mu = 4.73004074$

where $S_f(x) = \frac{\sinh(\mu x)}{\sinh(\frac{\mu}{2})} - \frac{\sin(\mu x)}{\sin(\frac{\mu}{2})}$, $S_f(z) = \frac{\sinh(\mu z)}{\sinh(\frac{\mu}{2})} - \frac{\sin(\mu z)}{\sin(\frac{\mu}{2})}$, $C_f(x) = \frac{\cosh(\mu x)}{\cosh(\frac{\mu}{2})} - \frac{\cos(\mu x)}{\cos(\frac{\mu}{2})}$, $C_f(z) = \frac{\cosh(\mu z)}{\cosh(\frac{\mu}{2})} - \frac{\cos(\mu z)}{\cos(\frac{\mu}{2})}$

Substituting eqn. (3.5) in eqn. (3.1), orthogonalizing with corresponding eigen function, integrating with respect to x and z between the limits $-\frac{1}{2}$ and $+\frac{1}{2}$ and following the usual procedure of stability we get Rayleigh number, (Ra) as follows:

$$Ra = \left[\frac{\langle \mathcal{G}_2(x,z)\nabla^2_{A_r}\mathcal{G}_2(x,z)\rangle}{(A_r)^5\left\langle \mathcal{G}_1(x,z)\frac{\partial}{\partial x}\mathcal{G}_2(x,z)\right\rangle}\right]\left[\frac{(1+N_1)\langle \mathcal{G}_1(x,z)\nabla^4_{A_r}\mathcal{G}_1(x,z)\rangle + N_1^2 X_1}{\left\langle \mathcal{G}_2(x,z)\frac{\partial}{\partial x}\mathcal{G}_1(x,z)\right\rangle - X_2}\right], \tag{3.6}$$

where

$$\langle \ldots \rangle = \int_{-\frac{1}{2}}^{\frac{1}{2}}\int_{-\frac{1}{2}}^{\frac{1}{2}} (\ldots)\, dz\, dx,$$

$$X_1 = \frac{\langle \mathcal{G}_1(x,z)\nabla^2_{A_r}\mathcal{G}_1(x,z)\rangle^2}{N_3\langle \mathcal{G}_1(x,z)\nabla^2_{A_r}\mathcal{G}_1(x,z)\rangle - 2N_1\langle \mathcal{G}_1(x,z)^2\rangle},$$

$$X_2 = \frac{N_1 N_5\langle \mathcal{G}_1(x,z)\nabla^2_{A_r}\mathcal{G}_1(x,z)\rangle\left\langle \mathcal{G}_2(x,z)\frac{\partial}{\partial x}\mathcal{G}_1(x,z)\right\rangle}{N_3\langle \mathcal{G}_1(x,z)\nabla^2_{A_r}\mathcal{G}_1(x,z)\rangle - 2N_1\langle \mathcal{G}_1(x,z)^2\rangle}.$$

The amount of heat transfer in the system cannot be determined with the help of linear stability-analysis. Therefore, in the next section, a weak non-linear analysis is performed to study heat transfer in the system using minimal representation of Fourier-series for stream function, micro-rotation and temperature. Through this, the physics of the problem can be well understood with simplified mathematical expression.

4. A Weak Non-Linear Analysis

The minimal-mode-representation to study weak non-linear analysis is taken as shown below. Comparing with the linear analysis two terms are considered in temperature in order to get the non-linearity:

$$\left.\begin{aligned} \Psi &= \mathcal{C}_1(t)\, \mathcal{G}_1(x,z), \\ \omega_y &= \mathcal{C}_2(t)\, \mathcal{G}_1(x,z), \\ T &= \mathcal{C}_3(t)\, \mathcal{G}_2(x,z) + \mathcal{C}_4(t)\, \mathcal{G}_3(z), \end{aligned}\right\} \tag{4.1}$$

where $\mathcal{C}_1$, $\mathcal{C}_2$, $\mathcal{C}_3$ and $\mathcal{C}_4$ are amplitudes (dependent on time) that are to be calculated from dynamics of system. $\mathcal{G}_1(x,z)$ and $\mathcal{G}_2(x,z)$ are taken as defined in Table 2 and $\mathcal{G}_3(z)$ is taken as $\sin(2\pi z)$ for all the three types of boundaries. Using eqn. (4.1) in eqn. (2.16) and orthogonalizing with respect to eigen functions we get the following non-linear autonomous Lorenz system:

$$\frac{d\mathcal{C}_1}{dt} = -\left[\frac{(1+N_1)I_3 Pr}{I_1}\right]\mathcal{C}_1 - [N_1 Pr]\,\mathcal{C}_2 - \left[\frac{Ra(A_r)^4 I_2 Pr}{I_1}\right]\mathcal{C}_3, \tag{4.2}$$

$$\frac{d\mathcal{C}_2}{dt} = -\left[\frac{N_1 I_1 Pr}{N_2 I_4}\right]\mathcal{C}_1 - \left[\frac{N_3 I_1 Pr}{N_2 I_4} - \frac{2N_1 Pr}{N_2}\right]\mathcal{C}_2, \tag{4.3}$$

$$\frac{d\mathcal{C}_3}{dt} = -\left[\frac{A_r I_6}{I_5}\right]\mathcal{C}_1 - \left[\frac{A_r I_6 N_5}{I_5}\right]\mathcal{C}_2 + \left[\frac{(A_r)^2 I_7 + I_8}{I_5}\right]\mathcal{C}_3 + \left[\frac{A_r I_9}{I_5}\right]\mathcal{C}_1\mathcal{C}_4 + \left[\frac{A_r I_9 N_5}{I_5}\right]\mathcal{C}_2\mathcal{C}_4, \tag{4.4}$$

$$\frac{d\mathcal{C}_4}{dt} = \left[\frac{I_{11}}{I_{10}}\right]\mathcal{C}_4 + A_r\left[\frac{I_{12} - I_{13}}{I_5}\right]\mathcal{C}_3\mathcal{C}_1 + A_r N_5\left[\frac{I_{12} - I_{13}}{I_5}\right]\mathcal{C}_2\mathcal{C}_3, \tag{4.5}$$

where

$$I_1 = \langle \mathcal{G}_1(x,z)\nabla^2_{A_r}(\mathcal{G}_1(x,z))\rangle, \quad I_2 = \left\langle \mathcal{G}_1(x,z)\frac{\partial}{\partial x}(\mathcal{G}_2(x,z))\right\rangle,$$

$$I_3 = \langle \mathcal{G}_1(x,z)\nabla^4_{A_r}(\mathcal{G}_1(x,z))\rangle, \quad I_4 = \langle(\mathcal{G}_1(x,z))^2\rangle, \quad I_5 = \langle(\mathcal{G}_2(x,z))^2\rangle,$$

$$I_6 = \left\langle \mathcal{G}_2(x,z)\frac{\partial}{\partial x}(\mathcal{G}_1(x,z))\right\rangle, \quad I_7 = \left\langle \mathcal{G}_2(x,z)\frac{\partial^2}{\partial x^2}(\mathcal{G}_2(x,z))\right\rangle,$$

$$I_8 = \left\langle \mathcal{G}_2(x,z)\frac{\partial^2}{\partial z^2}(\mathcal{G}_2(x,z))\right\rangle, \quad I_9 = \left\langle \mathcal{G}_2(x,z)\frac{\partial}{\partial x}(\mathcal{G}_1(x,z))\frac{\partial}{\partial z}\mathcal{G}_3(z)\right\rangle,$$

$$I_{10} = \langle(\mathcal{G}_3(z))^2\rangle, \quad I_{11} = \left\langle \mathcal{G}_3(z)\frac{\partial^2}{\partial z^2}(\mathcal{G}_3(z))\right\rangle, \quad I_{12} = \left\langle \mathcal{G}_3(z)\frac{\partial}{\partial x}(\mathcal{G}_1(x,z))\frac{\partial}{\partial z}(\mathcal{G}_2(x,z))\right\rangle,$$

$$I_{13} = \left\langle \mathcal{G}_3(z)\frac{\partial}{\partial z}(\mathcal{G}_1(x,z))\frac{\partial}{\partial x}(\mathcal{G}_2(x,z))\right\rangle.$$

5. Nusselt Number

The heat transfer is quantified by Nusselt number, $\mathcal{N}u(t)$ and is defined as:

$$\begin{aligned}\mathcal{N}u(t) &= \text{Heat transport by}\left[\frac{\text{conduction + convection}}{\text{conduction}}\right]\\ &= 1+\left.\frac{\int_{-\frac{1}{2}}^{\frac{1}{2}}\frac{\partial T}{\partial z}dx}{\int_{-\frac{1}{2}}^{\frac{1}{2}}\frac{dT_b}{dz}dx}\right|_{z=-\frac{1}{2}}\end{aligned} \tag{5.1}$$

On performing differentiation and integration in eqn. (5.1), by taking values of T from eqn. (2.12) and on solving Lorenz model in eqns. (4.2)–(4.5), we get the expression for $\mathcal{N}u(t)$ as:

Table 3. Nusselt number for different boundary conditions

F-F	R-F	R-R
$1+2\pi\mathcal{C}_4$	$1-4\pi\mathcal{C}_4$	$1+2\pi\mathcal{C}_4$

Average-Nusselt number, $\overline{\mathcal{N}u(t)}$ is calculated from $\mathcal{N}u(t)$ expression given in Table 3 for different boundaries using the following:

$$\overline{\mathcal{N}u(t)} = \frac{1}{t}\int_o^t (\mathcal{N}u(t))\,dt. \tag{5.2}$$

6. Results and Discussions

Linear and non-linear stability-analysis of Rayleigh-Bénard convection in three different types of enclosures filled with *micropolar fluid* (MPF) are studied in this paper. To investigate the problem, Free-Free, Rigid-Rigid and Rigid-Free conditions on boundaries of the enclosures are considered. Also, isothermal-horizontal and adiabatic-vertical boundaries with no-spin conditions are assumed in the problem. In the case of linear analysis, the stability of the system in three different enclosures are investigated through Ra, expressed as the function of A_r, N_1, N_3 and N_5. The amount of heat transfer in three different enclosures and boundaries are studied through $\overline{\mathcal{N}u(t)}$ by considering non-linear analysis.

Physically, the parameters A_r, Pr, N_1, N_3 and N_5 are respectively representing ratio of height to breadth of the enclosure (aspect ratio), relative measure of viscosity and heat conduction in a fluid flow (Prandtl number), concentration of micro-elements (coupling-parameter), micropolar-diffusion (couple-stress-parameter) and coupling of heat flux and spin (micropolar-heat-conduction-parameter). The range of N_1, N_3 and N_5 according to Clausius-Duhem-inequality are taken as $0 \le N_1 \le 1$, $0 \le N_3 \le a$ and $0 \le N_5 \le b$, where a and b are finite real numbers. Higher values of Pr is taken due to the presence of micro-elements. The value of A_r is taken in the range of $0.8 \le A_r \le 1.2$, with $A_r = 0.8$ for shallow, $A_r = 1$ for square and $A_r = 1.2$ for tall enclosure.

The impact of N_1, N_3 and N_5 on the on-set-of-convection is plotted in Figures 2–4 respectively for different boundaries and different enclosures. From Figure 2 we see that increase in N_1 increases Ra, micro-elements consume the major part of the energy to form circular motion in it's own axis and thereby on-set-of-convection is delayed. Figure 3 captures the effect of N_3 on Ra, it is noticed that with increase in N_3 decreases the micro-rotation of micro-elements, which advances the on-set-of-convection and thereby N_3 destabilizes the system. The impact of N_5 is given in Figure 4. As N_5 increases, heat induced into fluid by micro-elements also increases, which delays the convection, thus N_5 stabilizes the system.

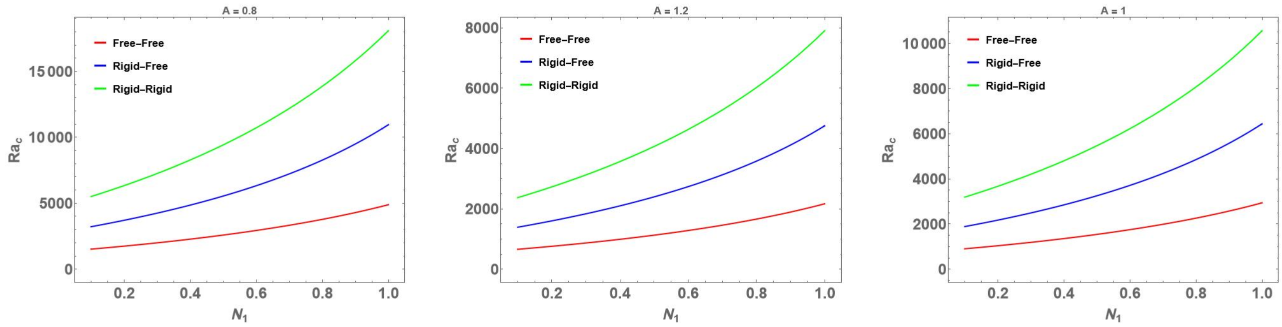

Figure 2. The impact of N_1 on Rayleigh-number for different boundaries

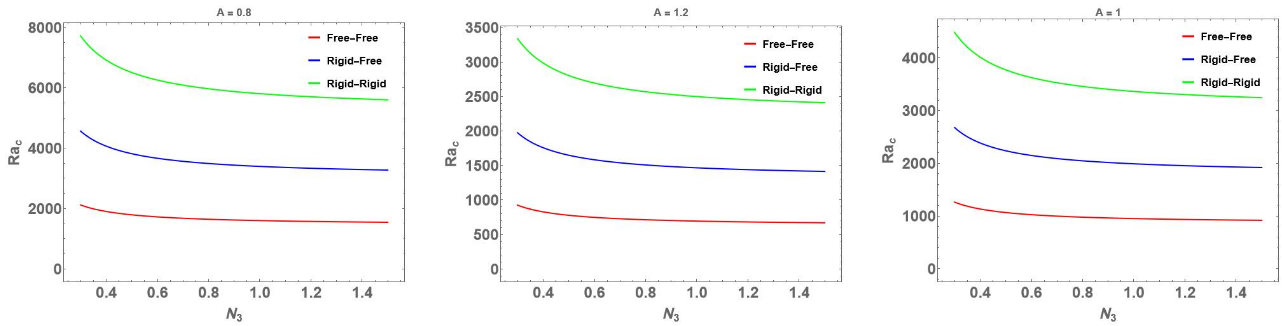

Figure 3. The impact of N_3 on Rayleigh-number for different boundaries

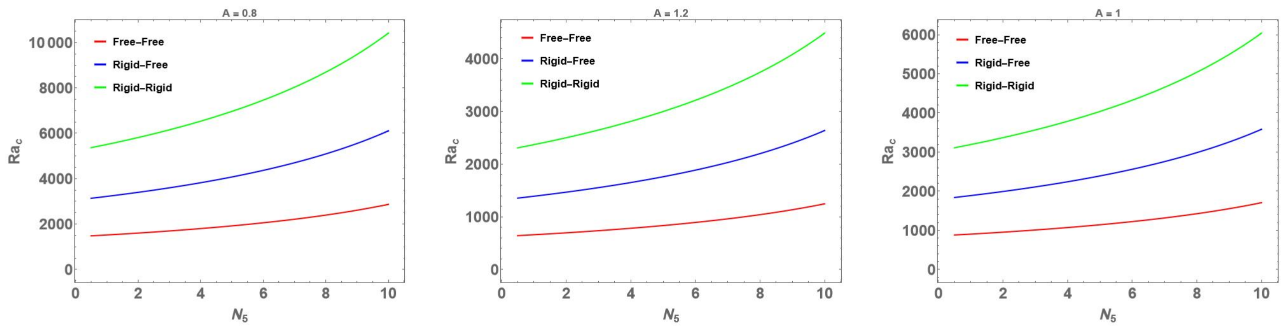

Figure 4. The impact of N_5 on Rayleigh-number for different boundaries

The above results can be summarized as:

(i) $Ra^{N_1=0.1} < Ra^{N_1=0.8}$

(ii) $Ra^{N_3=0.4} > Ra^{N_3=1.0}$

(iii) $Ra^{N_5=1.0} < Ra^{N_5=4}$

Also, following are observed from these figures:

(i) $Ra^{\text{R-R}} > Ra^{\text{R-F}} > Ra^{\text{F-F}}$

The above inequality shows that $R-R$ boundaries are more stable compared to the other two combinations of boundaries, due to their sticky nature.

(ii) $Ra^{A_r=0.8} > Ra^{A_r=1} > Ra^{A_r=1.2}$

The above shows that on-set-of-convection in shallow enclosure is delayed and in tall enclosure it advances. This is due to the fact that the energy supply from the lower plate is the same in all the three enclosures but the width of the lower plate on which this supply is made determines the extend of instability.

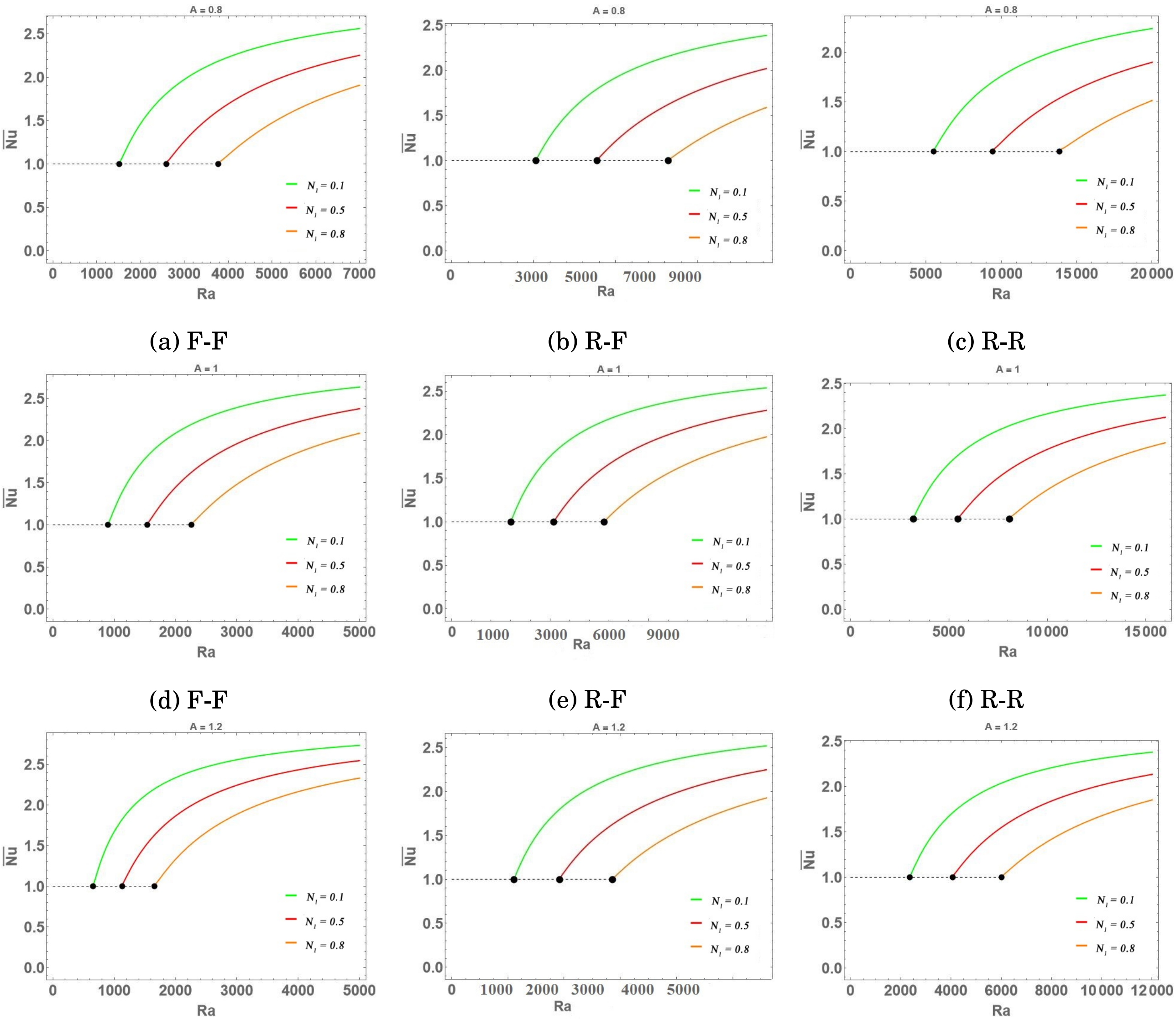

(a) F-F (b) R-F (c) R-R

(d) F-F (e) R-F (f) R-R

(g) F-F (h) R-F (i) R-R

Figure 5. The impact of $\overline{\mathcal{N}u(t)}$ on Rayleigh-number for variation of N_1 for different boundaries and enclosures

In this section, the findings from the non-linear analysis is discussed, which quantifies the heat transfer in terms of $\overline{\mathcal{N}u(t)}$. Figure 5 illustrates the amount of heat transport in different enclosures with the variation of N_1 for F-F, R-F and R-R boundaries, respectively. The following are observed from the subfigures:

(i) $\overline{\mathcal{N}u(t)}^{N_1=0.1} > \overline{\mathcal{N}u(t)}^{N_1=0.5} > \overline{\mathcal{N}u(t)}^{N_1=0.8}$, i.e., increase in the amount of micro-elements decreases $\overline{\mathcal{N}u(t)}$, this is because, increase in concentration of micro-elements stabilizes the system.

(ii) $\overline{\mathcal{N}u(t)}^{A_r=0.8} < \overline{\mathcal{N}u(t)}^{A_r=1.0} < \overline{\mathcal{N}u(t)}^{A_r=1.2}$, i.e., tall enclosures transport maximum heat on comparing with other (square and shallow) enclosures. This is due to the fact that tall enclosures requires less amount of energy in forming convection cell and thereby transfers more heat.

(iii) $\overline{\mathcal{N}u(t)}^{\text{R-R}} < \overline{\mathcal{N}u(t)}^{\text{R-F}} < \overline{\mathcal{N}u(t)}^{\text{F-F}}$, i.e., heat transport with R-R boundaries is less compared to R-F and F-F because for R-R boundaries, more energy is required to form convection cell thereby less energy is transported.

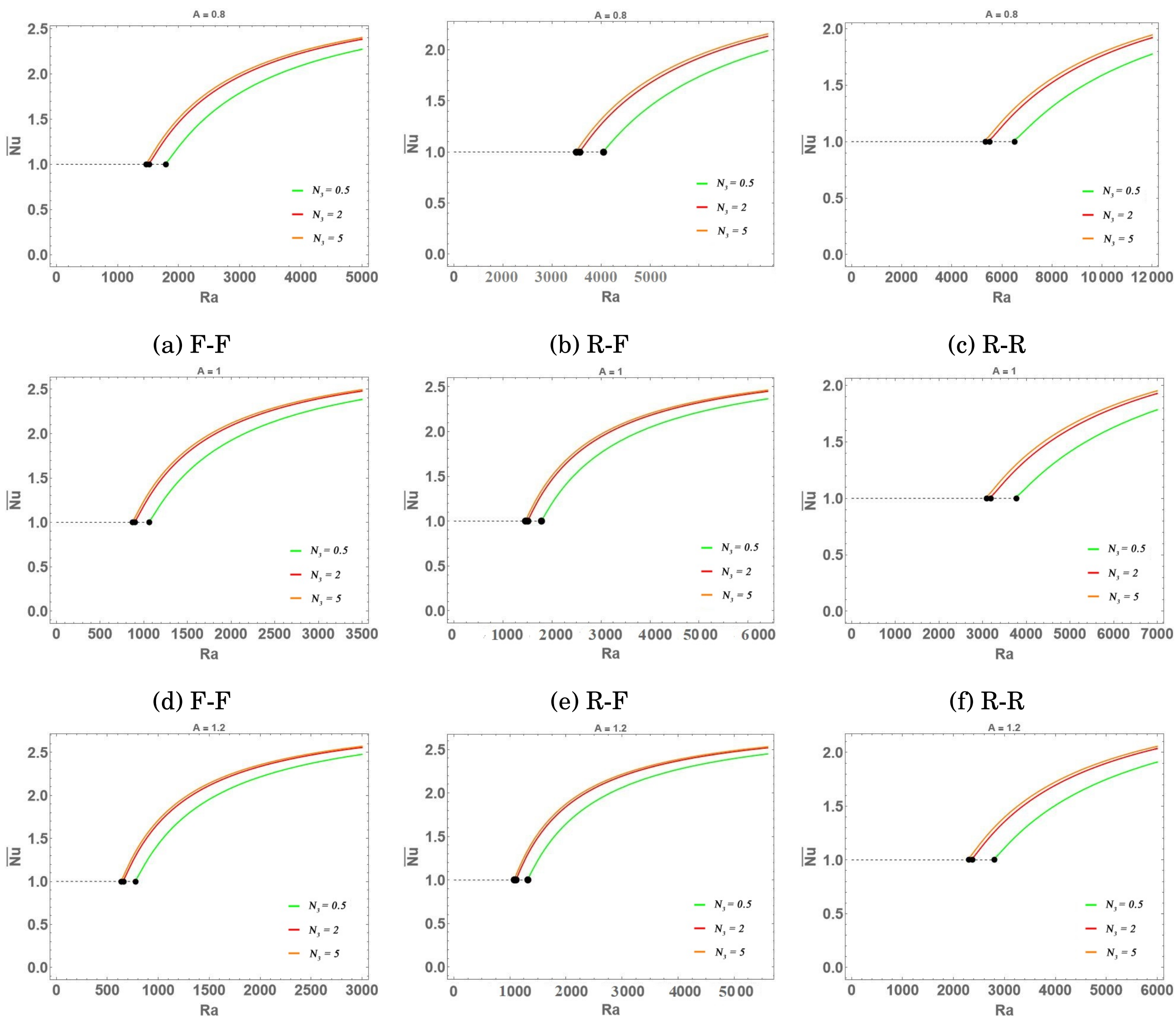

(a) F-F (b) R-F (c) R-R

(d) F-F (e) R-F (f) R-R

(g) F-F (h) R-F (i) R-R

Figure 6. The impact of $\overline{\mathcal{N}u(t)}$ on Rayleigh-number for variation of N_3 for different boundaries and enclosures

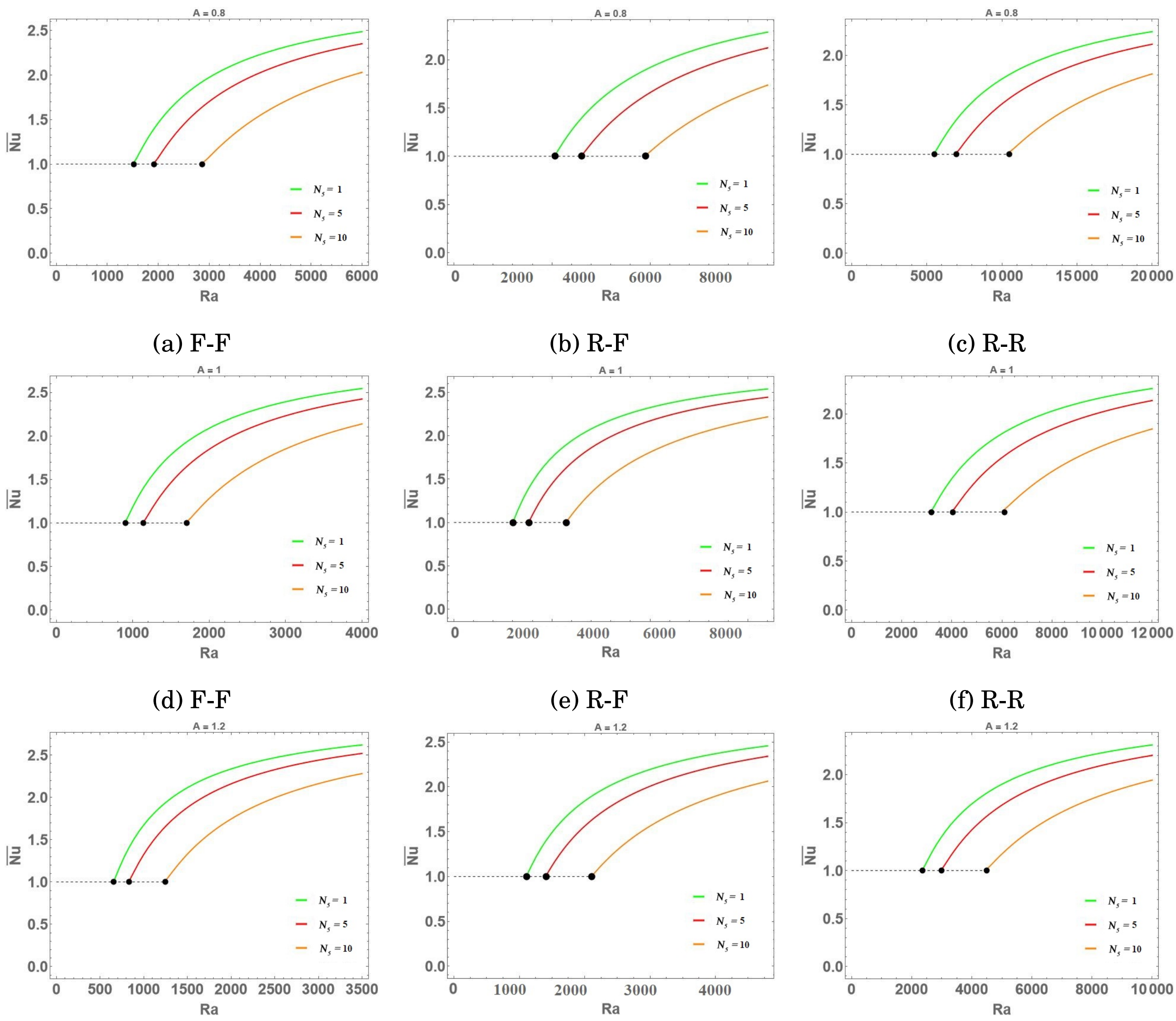

(a) F-F (b) R-F (c) R-R

(d) F-F (e) R-F (f) R-R

(g) F-F (h) R-F (i) R-R

Figure 7. The impact of $\overline{\mathcal{N}u(t)}$ on Rayleigh-number for variation of N_5 for different boundaries and enclosures

The impact of N_3 and N_5 on $\overline{\mathcal{N}u(t)}$ is studied from Figure 6 and Figure 7, respectively for all three types of boundary combinations. The following are observed:

(i) $\overline{\mathcal{N}u(t)}^{N_3=0.5} > \overline{\mathcal{N}u(t)}^{N_3=2} > \overline{\mathcal{N}u(t)}^{N_3=5}$

(ii) $\overline{\mathcal{N}u(t)}^{N_5=1} < \overline{\mathcal{N}u(t)}^{N_5=5} < \overline{\mathcal{N}u(t)}^{N_5=10}$

i.e. N_3 facilitates more heat transfer as it destabilizes the system and less heat transfer in N_5 as it stabilizes the system.

7. Conclusion

The present paper deals with analytical study of Rayleigh-Bénard convection in three types of enclosures and boundary combinations. The following are the main observations from the study:

(1) Addition of micro-elements with micro-structure to the Newtonian fluid increases the stability and thereby decreases the heat transport of the system.

(2) Shallow enclosure is more stable than square and tall enclosure which implies that heat transfer in tall enclosure is greater compared to square and shallow enclosure.

(3) Comparison of F-F, R-F, R-R boundary conditions, we conclude that F-F boundary is less stable compared to other two (R-F, R-R) and facilitates more heat transport.

(4) N_1 and N_5 stabilizes the system and decrease the heat transport, whereas increase in N_3 destabilizes the system and enhances the heat transport.

8. Conclusion

The study of Rayleigh-Bérnard convection in three types of enclosures and boundary combinations are carried out in micropolar fluid. Both the linear and non-linear analysis of the problem is investigated. When the amount of micro-elements increases, the system becomes more stable and thereby heat transfer is reduced. Shallow enclosure moves the system more stable on comparison with other two enclosures. On the other hand tall enclosure promotes more heat transfer than the square and tall enclosure. The micropolar fluid elements N_1 and N_5 helps in stabilizing the system and N_3 destablizes the system. The study on boundary condition shows that Rigid-Rigid boundary move the system stable and heat transfer is more in free-free boundary condition.

Competing Interests

The authors declare that they have no competing interests.

Authors' Contributions

All the authors contributed significantly in writing this article. The authors read and approved the final manuscript.

References

[1] G. Ahmadi, Stability of a micropolar fluid layer heated from below, *International Journal of Engineering Science* **14**(1) (1976), 81 – 89, DOI: 10.1016/0020-7225(76)90058-6.

[2] S. P. Bhattacharyya and S. K. Jena, On the stability of a hot layer of micropolar fluid, *International Journal of Engineering Science* **21**(9) (1983), 1019 – 1024, DOI: 10.1016/0020-7225(83)90043-5.

[3] M. Corcione, Effects of the thermal boundary conditions at the sidewalls upon natural convection in rectangular enclosures heated from below and cooled from above, *International Journal of Thermal Sciences* **42**(2) (2003), 199 – 208, DOI: 10.1016/S1290-0729(02)00019-4.

[4] A. B. Datta and V. U. K. Sastry, Thermal instability of a horizontal layer of micropolar fluid heated from below, *International Journal of Engineering Science* **14**(7) (1976), 631 – 637, DOI: 10.1016/0020-7225(76)90005-7.

[5] M. C. D'Orazio, C. Cianfrini and M. Corcione, Rayleigh–Bénard convection in tall rectangular enclosures, *International Journal of Thermal Sciences* **43**(2) (2004), 135 – 144, DOI: 10.1016/j.ijthermalsci.2003.05.002.

[6] A. C. Eringen, Simple microfluids, *International Journal of Engineering Science* **2**(2) (1964), 205 – 217, DOI: 10.1016/0020-7225(64)90005-9.

[7] A. C. Eringen, Theory of micropolar fluids, *Indiana University Mathematics Journal* **16**(1) (1966), 1 – 18, DOI: 10.1512/iumj.1967.16.16001.

[8] A. Y. Gelfgat, Different modes of Rayleigh–Bénard instability in two- and three-dimensional rectangular enclosures, *Journal of Computational Physics* **156**(2) (1999), 300 – 324, DOI: 10.1006/jcph.1999.6363.

[9] A. E. Gill, The boundary-layer regime for convection in a rectangular cavity, *Journal of Fluid Mechanics* **26**(3) (1966), 515 – 536, DOI: 10.1017/S0022112066001368.

[10] C. Kanchana, O. P. Suthar and P. G. Siddheshwar, A study of Rayleigh-Bénard-Taylor convection in very-shallow, shallow, square and tall enclosures, *International Journal of Applied and Computational Mathematics* **6** (2020), Article number: 78, DOI: 10.1007/s40819-020-00833-2.

[11] S. Kimura and A. Bejan, The boundary layer natural convection regime in a rectangular cavity with uniform heat flux from the side, *ASME Journal of Heat and Mass Transfer* **106**(1) (1984), 98 – 103, DOI: 10.1115/1.3246666

[12] S. A. Mikhailenko, I. V. Miroshnichenko and M. A. Sheremet, Thermal radiation and natural convection in a large-scale enclosure heated from below: Building application, *Building Simulation* **14** (2020), 681 – 691, DOI: 10.1007/s12273-020-0668-4.

[13] S. Ostrach, Natural convection in enclosures, *Advances in Heat Transfer* **8** (1972), 161 – 227, DOI: 10.1016/S0065-2717(08)70039-X.

[14] O. A. Olayemi, A.-F. Khaled, O. J. Temitope, O. O. Victor, C. B. Odetunde and I. K. Adegun, Parametric study of natural convection heat transfer from an inclined rectangular cylinder embedded in a square enclosuree, *Australian Journal of Mechanical Engineering* **21** (2) (2023), 668 – 681, DOI: 10.1080/14484846.2021.1913853.

[15] L. E. Payne and B. Straughan, Order of convergence estimates on the interaction term for a micropolar fluid, *International Journal of Engineering Science* **27**(7) (1989), 837 – 846, DOI: 10.1016/0020-7225(89)90049-9.

[16] Y. Qin and P. N. Kaloni, A thermal instability problem in a rotating micropolar fluid, *International Journal of Engineering Science* **30**(9) (1992), 1117 – 1126, DOI: 10.1016/0020-7225(92)90061-K.

[17] K. V. R. Rao, Thermal instability in a micropolar fluid layer subject to a magnetic field, *International Journal of Engineering Science* **18**(5) (1980), 741 – 750, DOI: 10.1016/0020-7225(80)90107-X.

[18] P. R. M. Santos, A. Lugarini, S. L. M. Junqueira and A. T. Franco, Natural convection of a viscoplastic fluid in an enclosure filled with solid obstacles, *International Journal of Thermal Sciences* **166** (2021), 106991, DOI: 10.1016/j.ijthermalsci.2021.106991.

[19] D. R. V. S. R. K. Sastry, N. N. Kumar, P. K. Kameswaran and S. Shaw, Unsteady 3D micropolar nanofluid flow through a squeezing channel: Application to cardiovascular disorders, *Indian Journal of Physics* **96** (2022), 57 – 70, DOI: 10.1007/s12648-020-01951-9.

[20] P. G. Siddheshwar and C. Kanchana, Unicellular unsteady Rayleigh-Bénard convection in Newtonian liquids and Newtonian nanoliquids occupying enclosures: New findings, *International Journal of Mechanical Sciences* **131–132** (2017), 1061 – 1072, DOI: 10.1016/j.ijmecsci.2017.07.050.

[21] P. G. Siddheshwar and S. Pranesh, Effect of temperature/gravity modulation on the onset of magneto-convection in weak electrically conducting fluids with internal angular momentum, *Journal of Magnetism and Magnetic Materials* **192**(1) (1999), 159 – 176, DOI: 10.1016/S0304-8853(98)00384-9.

[22] P. G. Siddheshwar and S. Pranesh, Magnetoconvection in a micropolar fluid, *International Journal of Engineering Science* **36**(10) (1998), 1173 – 1181, DOI: 10.1016/S0020-7225(98)00013-5.

[23] P. G. Siddheshwar and C. Siddabasappa, Unsteady natural convection in a liquid-saturated porous enclosure with local thermal non-equilibrium effect, *Meccanica* **55** (2020), 1763 – 1780, DOI: 10.1007/s11012-020-01198-y.

[24] P. G. Siddheshwar and T. S. Sushma, Reduction of a tri-modal Lorenz model of ferrofluid convection to a cubic-quintic Ginzburg-Landau equation using the center manifold theorem, *Differential Equations and Dynamical Systems* **2021** (2021), 1 – 19, DOI: 10.1007/s12591-021-00565-9.

[25] O. V. Trevisan and A. Bejan, Combined heat and mass transfer by natural convection in a vertical enclosure, *ASME Journal of Heat and Mass Transfer* **109**(1) (1987), 104 – 112, DOI: 10.1115/1.3248027.